Chapter 4: Spectroscopy

4.0 CW Spectroscopy

The BOOMERANG apparatus described in the last chapter measures a mechanical transient proportional to the sample's longitudinal magnetization. The oscillator-driving protocol used during this detection period relies on a nonlinear sweep in the frequency of an applied rf field. As we saw in Figure 3.16, the sweep has a center-band region during which the frequency change is slow. If this center-band region is near the Larmor frequency of spins in the sample, then the spins are inverted, and forces on the oscillator drive it into resonance. If the slow part of the sweep is far off the spin resonance then the driving field either never sweeps through resonance or it sweeps so quickly as to violate the adiabatic condition (Equation 3.6). In this case the applied field is ineffective in inverting the spins, and so no oscillator driving is observed. This suggests a simple procedure for measuring the NMR spectrum: cyclic adiabatic passage is applied to the spins, and the amplitude of the oscillator's trajectory is measured as a function of the frequency of the center-band, which is stepped on successive iterations of the experiment.

Figure 4.1 shows a graph of oscillator amplitude integrated over the detection time versus the center-band frequency of the applied field. These amplitudes clearly map out the frequency spectrum of the spin resonance. This

method can be viewed as a pointwise version of continuous-wave (CW) NMR spectroscopy. The spectrum shown in Figure 4.1 is that of protons in liquid water at 0.638 T.

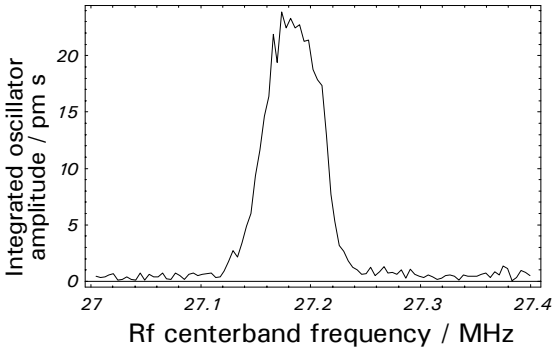

Figure 4.1. ^{1}H CW-NMR spectrum of liquid water.

The FWHM line width in this particular spectrum is 70 kHz, which is greater than the inhomogeneous linewidth of the liquid sample. This broadening is observed when the rf is strong enough to cyclically invert the spins even when the slow part of the sweep is somewhat off resonance. Because of this broadening effect, the cw spectrum is used only as a coarse measurement of the Larmor frequency.

4.1 Inversion-Recovery

Once the Larmor frequency is known, we can reproducibly measure the longitudinal magnetization of the sample by recording a transient and then fitting to find a signed amplitude. If the driving period follows a period during which this magnetization is modulated in some way, then one can measure relevant characteristics of the spin system. The simplest measurement that can be made in this way is of the longitudinal relaxation time, T_1. This is done using an inversion-recovery method.

Figure 4.2 shows a graph of integrated amplitude *vs.* the length of a time interval that follows a single adiabatic inversion and precedes detection. This interval t_1 is varied between iterations of the experiment, and on a given iteration the magnetization relaxes back toward equilibrium during t_1. The magnetization that survives this relaxation varies according to an exponential function. A fit to the graph yields the longitudinal relaxation time $T_1 = 1.67$ s for this sample, which is 1,1,1,3,3,3-hexafluoro-2-propanol ($(CF_3)_2CHOH$) at room temperature.

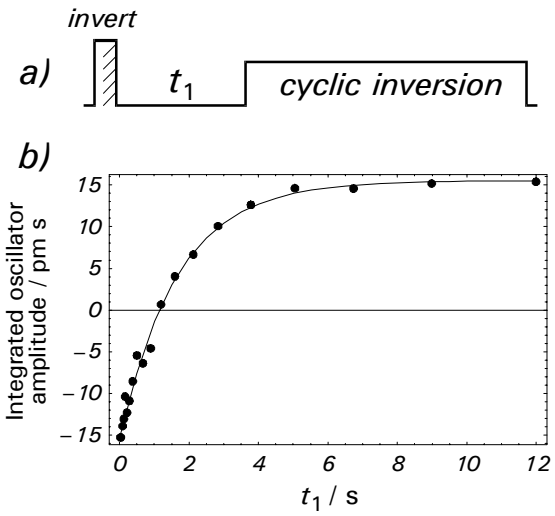

Figure 4.2. Measurement of ^{19}F T_1 by inversion-recovery. a) Pulse sequence. A single adiabatic inversion pulse is followed by an interval of variable length t_1. Then the oscillator's trajectory is measured during cyclic inversion. b) Integrated amplitude of the trajectory as a function of t_1. The sample is hexafluoroisopropanol. A fit to the exponential yields $T_1 = 1.67 \pm 0.1$ s.

4.2 Time Sequencing – FT-NMR with Half-Passages

This separation of a detection period from a time t_1 during which information about the spin system is encoded for measurement during detection is a general method with wide applicability. The detected observable, M_z, is often (except in susceptometry[1] and in inversion-recovery) not the one of interest. However, if one can apply pulses with well-defined flip angles to the sample, then it is a simple matter to use the detection of M_z to measure transverse magnetization. This is done

in pointwise fashion with time sequencing, which is also useful in optically[2] and inductively[3] detected NMR.

Figure 4.3 shows the most general scheme for encoding information about the magnetization into the oscillator's trajectory. The principle is to use the evolution period as a way to systematically create nonequilibrium longitudinal magnetization for measurement during detection. We have already seen one example of the longitudinal case (Figure 4.3 b), where the nonequilibrium magnetization is the result of incomplete longitudinal relaxation. If the detection period follows a single "store pulse" (with flip angle $\pi/2$), then the detection period instead measures a single component of *transverse* magnetization.

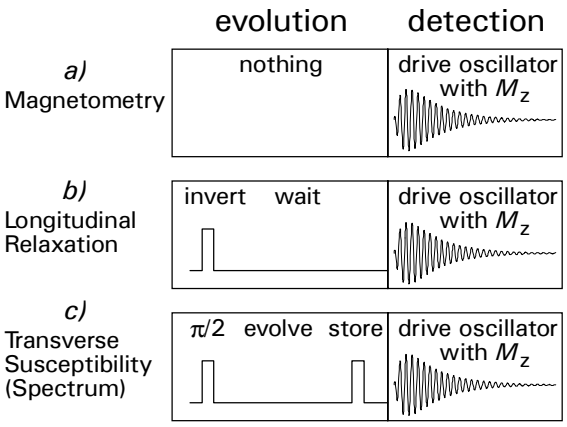

Figure 4.3. Time sequencing for pointwise acquisition of information from spin systems. The detection period is preceded by an evolution period during which information about the sample is encoded into non-equilibrium magnetization. Aspects of the evolution period are varied between iterations of the experiment.

This is illustrated by a simple pulse sequence that can be used to measure FT-NMR, which is shown in Figure 4.3 c. The initial $\pi/2$ pulse creates transverse magnetization from equilibrium magnetization. This transverse magnetization precesses in the static field for a measured time t_1. During this period, the spins evolve under the influence of the total spin Hamiltonian, whose dominant term is due to the static field, but which also includes chemical shift, field inhomogeneity,

and spin-spin couplings. After t_1 has elapsed, a second $\pi/2$ pulse is applied. This pulse selects one component of the transverse magnetization that survives the evolution interval for measurement during the detection period. The integrated amplitude of the detected transient is recorded as a function of t_1, and the length of this interval is varied on successive iterations of the experiment. The resulting time-domain signal is subject to Fourier transformation, yielding the spectrum.

This protocol relies on pulses with well-defined flip angles. Such flip angles can be measured with a nutation pulse sequence as described in section 4.3. This nutation sequence in turn requires that an accurate Larmor frequency has already been established, so that the frequency offset used is small compared to the Rabi frequency.

A simple way to circumvent this difficulty is to perform FT-NMR with the pulse sequence of Figure 4.3 b, but with the $\pi/2$ pulses replaced by adiabatic half-passages. If an adiabatic sweep is terminated in the center of the NMR line (when $\Delta = 0$, see Figure 3.15) the sample's magnetization is left in the transverse plane with a well-defined phase. The rf is turned off and then, after t_1 has elapsed, it is turned back on again with the same frequency and phase. If the adiabatic sweep is resumed to completion, then this procedure selects one component of the transverse magnetization that survives evolution during t_1 for subsequent detection. The size of the signal is relatively insensitive to the exact Larmor frequency (a previous measurement with CW spectroscopy suffices), and one requires only a very rough estimate of the Rabi frequency for use in selecting tangent sweep parameters.

Figure 4.4 shows an FT-NMR spectrum of liquid water obtained in this way. The observed spectrum is not subject to power-broadening as it is in CW spectroscopy, and so the NMR line is substantially narrower. The resulting better estimate of the Larmor frequency can be used in nutation and subsequently in multiple-pulse experiments. The line width is dominated by residual inhomogeneity in the static field. It is to be emphasized that this left-over inhomogeneity (which is about three orders of magnitude less than it would be were the annular magnets removed) is well within the range of compensation by mechanical or electrical shimming apparatus, which have not been included in the prototype.

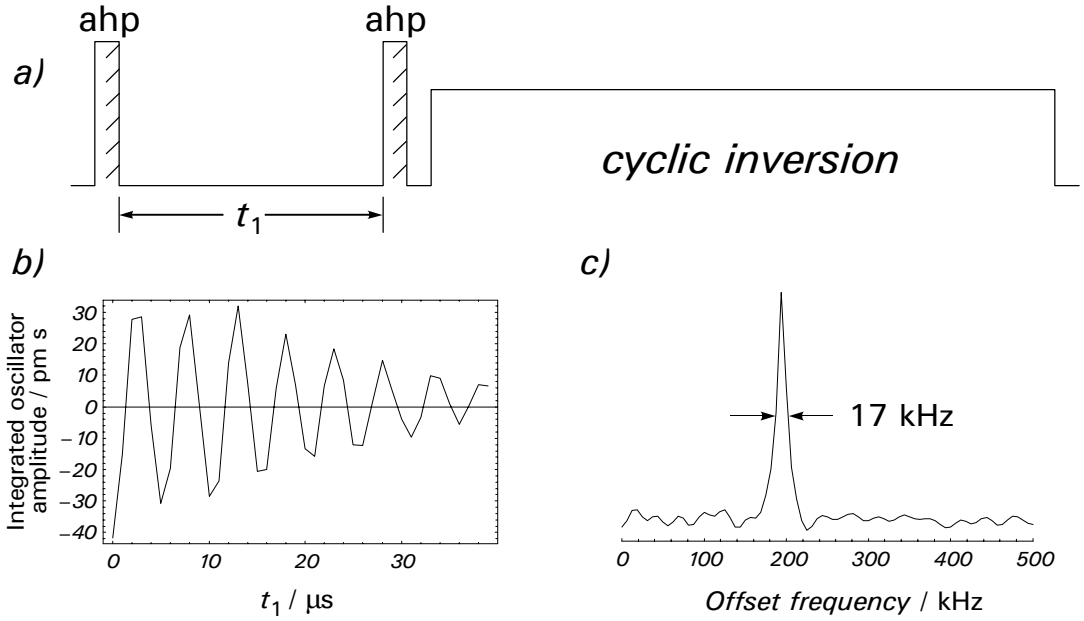

Figure 4.4. FT-NMR with adiabatic half-passages. a) Pulse sequence. An adiabatic half-passage creates transverse magnetization, which evolves during t_1. A store pulse selects one component of this magnetization, which is used to drive the oscillator during cyclic inversion. b) Integrated amplitude of the oscillator's trajectory as a function of t_1. This time-domain signal can be Fourier-transformed to yield a spectrum. c) The NMR spectrum. Data in (b) were fit to an exponentially decaying cosine, and this fitting function was used to extend the time-domain data (by a factor of four) in lieu of apodization in order to suppress noise and artifacts of the Fourier transform.

This method of encoding evolution of transverse magnetization (the single-quantum spectrum) into pointwise evolution of M_z bears resemblance to how multiple-quantum coherences are encoded pointwise into observable transverse magnetization in two-dimensional NMR spectroscopies[4]. In principle, *any* NMR pulse sequence can be inserted into the evolution interval in BOOMERANG. The separation of encoding and detection into distinct time intervals in BOOMERANG allows the whole spectrum to be obtained even though the spectral bandwidth is orders of magnitude larger than the oscillator bandwidth.

4.3 Nutation – t_1 and t_2 Noise

Figure 4.5 a shows a pulse sequence that can be used to measure the Rabi frequency of spins in the applied rf field (by nutation of the magnetization). The Rabi frequency is obtained by fitting the data in Figure 4.5 b to a decaying exponential or by Fourier transformation. The signal-to-noise in this experiment is sufficient to obtain a Rabi frequency to within about 5% (standard error). Figure 4.5 c shows residuals from the fit. The rms deviation in each time-domain point is about 6.9 pm, which is substantially larger than the ~0.5 pm rms error one would predict from the observed statistics of the t_2 transients given the ~0.5-Hz bandwidth of the measurement. The t_1 noise is therefore about 15 times larger than the t_2 noise. A similar analysis can be performed on data from the CW-NMR experiment shown in Figure 4.1. In that case, phases are not used at all in the fits, and the measured rms t_1 noise in each point's absolute value is about 0.3 pm. This shows that instabilities in the phase of the signal are at present our main noise source. Part of this phase instability comes from changes in the oscillator frequency during the driving interval,

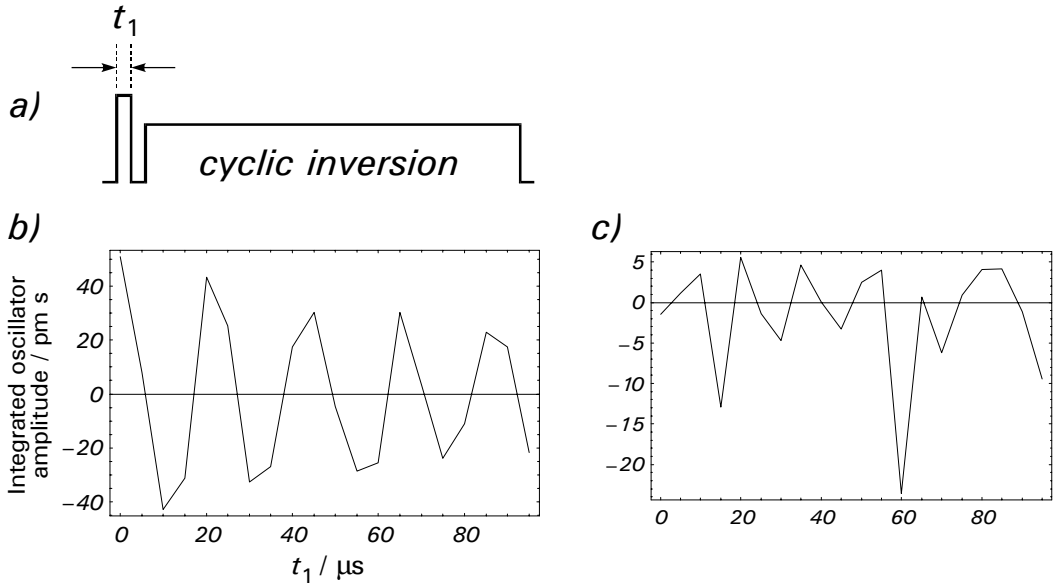

Figure 4.5. Nutation of proton magnetization in water. a) Pulse sequence. A single rf pulse of varied length t_1 is applied, followed by cyclic inversion and detection of the oscillator's trajectory. b) Integrated amplitude of the oscillator's trajectory as a function of t_1. A fit to an exponentially decaying cosine shows that the Rabi frequency is 46.7 ± 0.2 kHz. c) Residuals from the fit. The noise is about 20 times larger than what one would calculate from the noise in the transients. The t_1 noise is probably from instabilities in phase shot-to-shot in the experiment.

as we observed in Chapter 3. But it was also observed that the software triggering of the data acquisition in the prototype was subject to considerable jitter. Indeed, removal of the single point in the nutation time-domain data at $t_1 = 60\,\mu s$ reduces the rms errors by almost a factor of two. A look at the phase reference channel for this point shows substantial shift relative to other points.

4.4 Spin Echo

After relatively precise Larmor and Rabi frequencies are obtained from FT-NMR and nutation, in principle any multiple-pulse NMR experiment is compatible

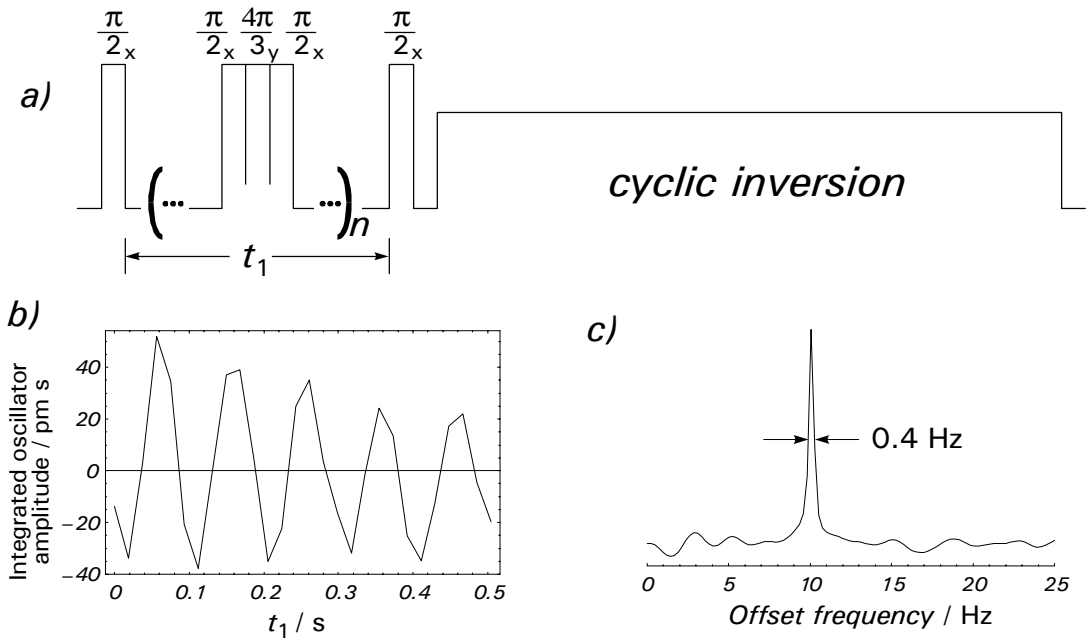

Figure 4.6. ^{19}F spin echo in hexafluoroisopropanol. a) Pulse sequence. A train of compensated π pulses is applied between a preparatory π/2 pulse and a "store pulse." b) Integrated amplitude of the oscillator's trajectory as a function of t_1. A fit to an exponentially decaying cosine is used, and the decay time is 0.96 ± 0.3 s. This fitting function is used to extend the time-domain data (by a factor of eight) in lieu of apodization in order to suppress artifacts of the Fourier transform. The resulting Fourier spectrum (c) exhibits a FWHM linewidth of 0.4 Hz.

with BOOMERANG. Figure 4.6 shows an example, a spin-echo sequence applied to ^{19}F in hexafluoroisopropanol using a train of composite π pulses. The decay time of the echo transient (0.96 s) is comparable to but somewhat smaller than the T_1 observed in the same compound by inversion-recovery (1.67 s). Given that the intrinsic rotating-frame relaxation time ($T_{1\rho}$) of the sample is likely near T_1 for such a small molecule, there are at least three factors that might contribute to this increased decay time. Some dephasing is probably taking place due to imperfections in the pulses. Such dephasing was not refocused because limitations in the pulse-programming hardware prevented phase-cycling the echo sequence. Another

possibility is dephasing due to diffusion in the residual gradient. Finally, the apparent signal strength itself may also be decreasing due to changes in the oscillator or in the Larmor frequency due to a slight drift in the sensor's magnetization.

4.5 Heteronuclear J Spectroscopy

Figure 4.7 shows an experiment with pulses on 2 nuclei (^{1}H and ^{19}F) in fluoroacetonitrile (FCH_2CN). The composite π pulses that were used in the echo experiment of Figure 4.6 were applied to both ^{1}H and ^{19}F after a preparatory $\pi/2$ pulse on ^{1}H. The time delay is incremented iteration to iteration in the experiment as always. When composite π pulses are applied to both spins, chemical shift and field inhomogeneity terms in the Hamiltonian are refocused, but the heteronuclear scalar coupling is not. The scalar coupling is observed in the spectrum as a splitting.

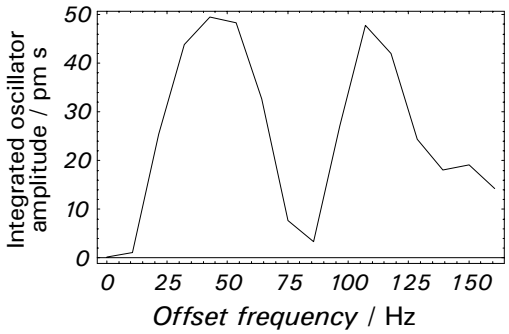

Figure 4.7. Heteronuclear J spectrum of fluoroacetonitrile. A train of compensated π pulses was applied to both ^{19}F and ^{1}H between a preparatory $\pi/2$ pulse and a store pulse on ^{1}H.

References

1 L. A. Madsen, Ph. D. Thesis, California Institute of Technology, 2002.

2 S. K. Buratto, D. N. Shykind, and D. P. Weitekamp, *Phys. Rev. B* **44,** 9035 (1991).

3 D. P. Weitekamp, *Adv. Magn. Reson.* **11,** 111 (1983).

4 R. R. Ernst, G. Bodenhausen, and A. Wokaun, *Principles of Nuclear Magnetic Resonance in One and Two Dimensions* (Clarendon Press, Oxford, 1987).